TECHNICAL REPORT
NATICK/TR-17/021

AD _____

INTEGRATED PROTECTIVE FABRIC SYSTEM (IPFS) PHASE III PROGRAM: AEROSOL PROTECTION REPORT

by
Walter Zukas
Natalie Pomerantz
Joseph Venezia
and
Michael Sieber

August 2017

Final Report
October 2013 – September 2015

Approved for public release; distribution is unlimited

U.S. Army Natick Soldier Research, Development and Engineering Center
Natick, Massachusetts 01760-5000

DISCLAIMERS

The findings contained in this report are not to be construed as an official Department of the Army position unless so designated by other authorized documents.

Citation of trade names in this report does not constitute an official endorsement or approval of the use of such items.

DESTRUCTION NOTICE

For Classified Documents:

Follow the procedures in DoD 5200.22-M, Industrial Security Manual, Section II-19 or DoD 5200.1-R, Information Security Program Regulation, Chapter IX.

For Unclassified/Limited Distribution Documents:

Destroy by any method that prevents disclosure of contents or reconstruction of the document.

REPORT DOCUMENTATION PAGE

Form Approved
OMB No. 0704-0188

1. REPORT DATE *(DD-MM-YYYY)*	2. REPORT TYPE	3. DATES COVERED *(From - To)*
16-08-2017	Final	October 2013 – September 2015

4. TITLE AND SUBTITLE

INTEGRATED PROTECTIVE FABRIC SYSTEM (IPFS) PHASE III PROGRAM: AEROSOL PROTECTION REPORT

5a. CONTRACT NUMBER

5b. GRANT NUMBER

5c. PROGRAM ELEMENT NUMBER

6. AUTHOR(S)

Walter Zukas, Natalie Pomerantz, Joseph Venezia, and Michael Sieber

5d. PROJECT NUMBER
BA07PRO102

5e. TASK NUMBER

5f. WORK UNIT NUMBER

7. PERFORMING ORGANIZATION NAME(S) AND ADDRESS(ES)

U.S. Army Natick Soldier Research, Development and Engineering Center
ATTN: RDNS-SEW-TMC
10 General Greene Avenue, Natick, MA 01760-5000

8. PERFORMING ORGANIZATION REPORT NUMBER

NATICK/TR-17/021

9. SPONSORING / MONITORING AGENCY NAME(S) AND ADDRESS(ES)

Defense Threat Reduction Agency
8275 John J. Kingman Rd.
Stop 6201
Fort Belvoir, VA 22060-6201

10. SPONSOR/MONITOR'S ACRONYM(S)
DTRA

11. SPONSOR/MONITOR'S REPORT NUMBER(S)

12. DISTRIBUTION / AVAILABILITY STATEMENT

Approved for public release. Distribution is unlimited.

13. SUPPLEMENTARY NOTES

14. ABSTRACT

This report addresses the characterization of aerosol performance of the individual materials and the layered structures of the five garment design concepts developed in the Integrated Protective Fabric System (IPFS) program at the U.S. Army Natick Soldier Research, Development and Engineering Center together with two chemical biological (CB) ensemble control configurations. Aerosol protection is an important feature in the development of the next generation CB protective ensemble. Understanding the relationships between material properties, ensemble design, and ensemble aerosol system performance is essential for this development. Material swatch testing was carried out to determine the filtration efficiency of the garment materials. Aerosol system tests were carried out on the configurations to determine aerosol deposition velocities on the skin which were then used in Body Region Hazard Analysis (BRHA) models to determine local and systemic ranking for the configurations. Configurations both better and worse than the controls were identified with significance depending on the data set considered and the BRHA model employed. Generally, two layer designs showed greater aerosol protection when compared to the one layer control. It was observed that aerosol swatch measurements showed no correlation to aerosol system test performance for the materials and configurations investigated in this study.

15. SUBJECT TERMS

AEROSOLS CB PROTECTION AEROSOL SYSTEM TEST AEROSOL PENETRATION
FILTRATION AEROSOL DEPOSITION PROTECTIVE CLOTHING CHEMICAL PROTECTION
PROTECTION DEPOSITION VELOCITY TEST AND EVALUATION FILTRATION EFFICIENCY
PENETRATION AEROSOL PROTECTION BODY REGION HAZARD ANALYSIS
CHEMICAL PROTECTIVE GARMENT

16. SECURITY CLASSIFICATION OF:			17. LIMITATION OF ABSTRACT	18. NUMBER OF PAGES	19a. NAME OF RESPONSIBLE PERSON
a. REPORT	b. ABSTRACT	c. THIS PAGE			Walter Zukas
U	U	U	UU	48	19b. TELEPHONE NUMBER *(include area code)* 508-233-5656

This page intentionally left blank

TABLE OF CONTENTS

LIST OF FIGURES

LIST OF TABLES

EXECUTIVE SUMMARY

This report addresses the characterization of aerosol protection performance of the individual materials and the layered structures of the five garment design concepts developed in the Integrated Protective Fabric System (IPFS) program at the U.S. Army Natick Soldier Research, Development and Engineering Center (NSRDEC) together with two chemical biological (CB) ensemble control configurations, during the period from October 2013 to September 2015. This report is one of multiple reports being prepared on the IPFS program, which culminated with a field demonstration of the concept configurations in 2014. The other reports being prepared address material development and selection, material manufacturing, omniphobic property development and measurement, thermal properties and comfort, ensemble modeling, and reactive material development for protection. Aerosol protection is an important feature in the development of the next generation CB protective ensemble. Understanding the relationships between material properties, ensemble design, and ensemble aerosol system performance is essential for this concept development.

Material swatch testing was carried out through a contract with Battelle Memorial Institute and also at NSRDEC to determine the filtration efficiency of the garment materials. The contracted work consisted of the aerosol performance characterization of the full assembly of material layers. Aerosol swatch testing at NSRDEC was conducted to confirm the contracted results and to characterize some of the separate material layers used as part of the full configuration. The contracted work was carried out over a range of aerosol particle sizes from 0.09 to 2.3 μm while the instrumentation at NSRDEC was limited to the larger size of 0.8 μm. In general, good agreement was found between the two methods for the smaller particle sizes investigated (0.1 to 0.3 μm), which also correspond to the most penetrating particle sizes and the particle size specified in the Technology Transition Agreement (TTA). A ranking of the configurations by swatch filtration efficiency was then established.

The NSRDEC swatch instrumentation was also used to explore the durability of the configurations through laundering. Swatches of configuration sub-assemblies containing aerosol barrier layers that were laundered clearly showed a decrease in filtration efficiency. Laundering caused delamination of the expanded polytetrafluoroethylene (ePTFE) aerosol barrier layer used in some garment configurations, and the thinner barrier layers exhibited greater filtration efficiency reductions.

Aerosol system tests (ASTs) were carried out through a contract at Research Triangle Institute (RTI) on the five full configurations of the IPFS garment designs and the two baseline garment controls. Aerosol deposition velocities were determined through skin rinse methods and were used in Body Region Hazard Analysis (BRHA) models to determine the local and systemic performance of the configurations. Five replicates of each configuration were run, and statistical analysis was conducted to identify significant differences between the IPFS configurations and the controls. Configurations both better and worse than the controls were identified with statistical significance depending on the data set considered and the BRHA model employed.

It was observed that aerosol swatch measurements showed no correlation to aerosol system test performance for the materials and configurations investigated in this study.

INTEGRATED PROTECTIVE FABRIC SYSTEM (IPFS) PHASE III PROGRAM: AEROSOL PROTECTION REPORT

1. INTRODUCTION

This report addresses the aerosol protection characteristics of the materials and garment systems investigated as part of the Integrated Protective Fabric System (IPFS) project at the U.S. Army Natick Soldier Research, Development and Engineering Center (NSRDEC) and covers the period from October 2013 to September 2015. The testing consisted of aerosol swatch testing at NSRDEC and Battelle and of configuration system testing at Research Triangle Institute (RTI). These tests are described in more detail in the Experimental Section chapter and the Results and Discussion chapter in this report. The goals of the aerosol studies were to determine if statistically significant differences could be observed between the configurations in aerosol performance through system testing and if swatch level testing could be used in combination with garment design to predict system-level results. The ultimate goal is to use the information gained from this range of materials and garment designs to provide a basis for improved aerosol protection of future garment systems.

The key reference for much of the data in this aerosol report is the Defense Technical Information Center (DTIC) available report titled, "Final Report Integrated Protective Fabric System Candidate Barrier Materials Chemical Agent and Simulant Testing" (McVeety et al., 2015). This report includes a description of the materials and material controls, a description of the IPFS configurations, details on the Battelle aerosol swatch testing, and the RTI-contracted system test report. Excerpts from the McVeety et al. reference will be utilized in sections of this report to clarify particular points, but the detailed full descriptions are available in this reference. Henceforth, this reference will be referred to as the "Battelle report".

In addition to this aerosol report, separate IPFS reports are in preparation which will address the topics of material selection, omniphobic properties, thermal properties, incorporating reactive materials, manufacturing of layered structures and garments, and modeling. This report will reference the materials and manufacturing reports for greater technical detail rather than repeating the information.

1.1 Technology Transition Agreement (TTA) for IPFS

A TTA for IPFS to Uniform Integrated Protective Ensemble 2 (UIPE 2) was established in July 2012 to define the technology parameters that will be designed, developed, demonstrated, and transitioned by the IPFS project to the next generation protective fabric system for use as a – chemical biological (CB) protective garment. The performance criteria for swatch and system-level testing pertaining to aerosols are shown in **Table 1**. The current baseline performance levels are adopted from the Joint Service Lightweight Integrated Suit Technology (JSLIST) system requirements and are quantified in **Table 1** under the "Current" column. "Threshold" values are associated with the Joint CB Coverall for Combat Vehicle Crewmen (JC3). The testing addressed in this report was typically carried out over a range of conditions, including

swatch and system measurements at the conditions shown in **Table 1**. This broader range is also addressed in later chapters of the report (Sections 3.1, 3.2, and 3.5).

Table 1. Aerosol Performance Thresholds and Objectives

Properties	**Current**	**Threshold**	**Objective**
Aerosol filtration efficiency (swatch) [filtration of 100 nm particle @ 1.8 cm/s face velocity(corresponds to 10 mph wind)]	70%	90%	97%
Aerosol System Test (AST) – Total surface dose 10 mph, 30 min @ 5000 mg·min/m^3	Same as JSLIST	Same as JC3	Meet toxic endpoints for advanced threats

1.2 IPFS Configurations

Five concept CB individual protection suits were developed as part of the IPFS program to address a range of mission scenarios. These concept configurations will be described in detail in the concurrent IPFS Materials Report and the IPFS Materials Manufacturing Report and are briefly reviewed here. These configurations are shown in **Figure 1** with the notations of C1 through C5, which will be used throughout this report. In addition to these five concept configurations, two control configurations, based on the JSLIST, were utilized for both material and system comparisons. The control configurations will be referred to as C6 and C7 throughout this report and are also included in the brief configuration descriptions that follow.

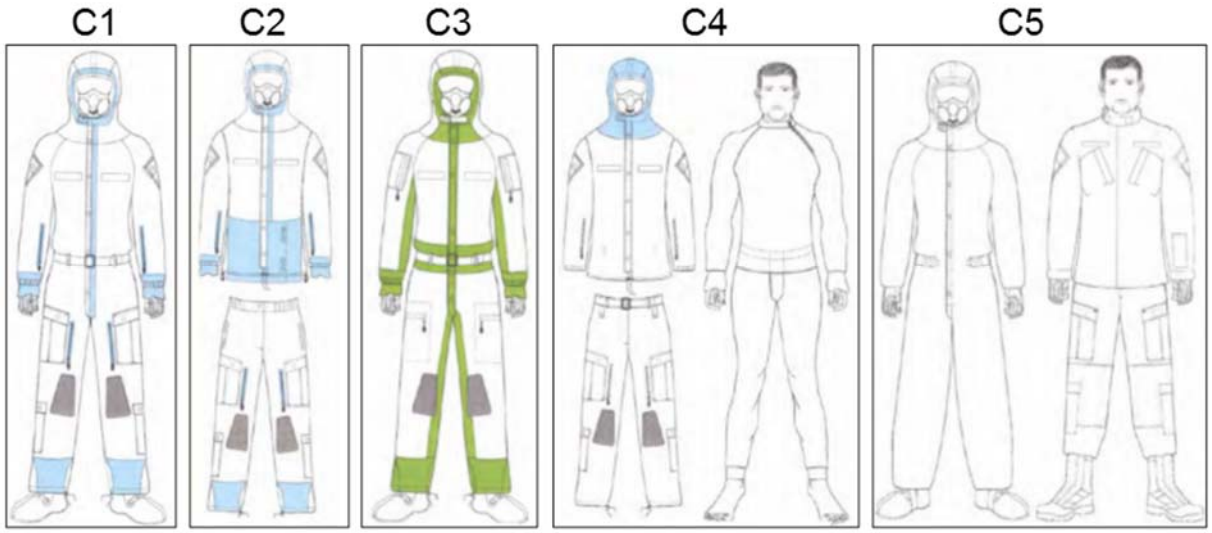

Figure 1. IPFS concept configurations

The C1 configuration is designed as a continuous use, one-piece coverall with inherent CB protection. It would be worn in place of a combat uniform. The air-permeable protective material system consists of a cover fabric laminated to an aerosol membrane with a separate sorptive

material layer with additional sorptive material at critical interfaces and closures. This configuration is also referred to as the CB Combat Coverall-A (CBCC-A).

The C2 configuration is designed as a continuous use, two-piece coverall with inherent CB protection. It would be worn in place of a combat uniform. The materials are the same as those used in the C1 configuration. This configuration is also referred to as the CB Flame Resistant (FR) Army Combat Uniform (CBFRACU).

The C3 configuration is designed as a continuous use, one-piece coverall with inherent CB protection. It would be worn in place of a combat uniform. The primary material contains an air-impermeable, self-detoxifying, and permselective membrane with air-permeable sorptive materials used at critical interfaces, closures, and passive vents. This configuration is also referred to as the CB Combat Coverall-B (CBCC-B).

The C4 configuration is designed as a combination of a continuous use undergarment and combat uniform with inherent CB protection. The undergarment consists of a separate sorptive material layer. The enhanced combat uniform consists of a cover fabric laminated to an aerosol membrane with a separate sorptive layer where the undergarment does not cover (i.e., hood). The two parts of this configuration are also referred to as the Enhanced Flame Resistant Army Combat Uniform (EFRACU) worn over a CB Undergarment (CBUG).

The C5 configuration is designed as an emergency use coverall with inherent CB protection worn over a combat uniform. The air-permeable protective coverall consists of a woven cover fabric laminated to a nonwoven aerosol membrane with an embedded sorptive material. The two parts of this configuration are also referred to as the CB Emergency Coverall (CBEC) worn over an FR Army Combat Uniform (FRACU)

The C6 configuration is the JSLIST and is used in this study as a CB control. It consists of a woven nylon/cotton outer shell ripstop fabric with a durable water repellent finish (Quarpel) with a hung liner comprised of a sorptive layer laminated to an inner tricot knit back.

The C7 configuration is the JSLIST worn over a FRACU and is also used in this study as a CB control.

Garment configurations C1, C2, C3, and C4 all incorporate novel closures and designs to improve chemical and aerosol resistance while providing means to decrease thermal burden. This is accomplished through strategically placed sorptive materials, seam design, and incorporation of closable vents in the regions shown as shaded/highlighted areas in **Figure 1**. Garment configuration C5 and the CB baselines C6 and C7 contain current closure designs and garment features. More detail on the specific design elements incorporated into each configuration can be found in the Battelle report.

Further detail on the specific materials used in each of the configurations is discussed in the Experimental Section of this report.

2. EXPERIMENTAL SECTION

2.1 IPFS Materials and Controls

Each of the garment configurations shown in **Figure 1** incorporate different layers of materials in order for the resulting system properties to meet the function for which they were designed. The material layers and finishes investigated in this study fall into general function categories (repellent finishes, shell fabrics, aerosol membranes, reactive membrane, and sorptive materials) and are listed below. One material, Tax-Shield Saratoga #101765, is a laminated fabric system consisting of a shell fabric with a carbon bead impregnated polypropylene (PP) aerosol membrane and appears in the multiple function categories that apply. A separate IPFS materials report, corresponding to this aerosol report, is in preparation as a technical report and will cover the material structure and selection in more detail.

Repellent finishes

- Luna UltraEverShield
- Luna UltraEverShield with 8-hydroxyquinoline/benzisothiazol (8-HQ/BIT)
- JSLIST Quarpel

Shell fabrics

- Sigma 4 Star ripstop woven fabric
- Sigma Versatech FR ripstop woven fabric
- Tencate Defender M FR
- Tencate Defender M Stretch FR woven fabric
- Tex-Shield Saratoga #101765 laminated fabric system has a woven cotton/polyester shell fabric
- JSLIST nylon/cotton ripstop

Aerosol membranes

- Stedfast Stedair TX3109 expanded polytetrafluoroethylene (ePTFE) membrane (light)
- Stedfast Stedair TX3114 ePTFE membrane (heavy)
- Tex-Shield Saratoga #101765 laminated fabric system has a PP aerosol membrane.

Reactive membrane

- Stedfast polyvinyl amine (PVAM) with 8-HQ/BIT

Sorptive materials

- Calgon Zorflex activated carbon cloth
- Stedfast StedCarb activated carbon cloth
- Tex-Shield Saratoga Stretch #103774 sorptive fabric
- Tex-Shield Saratoga #101765 laminated fabric system has carbon bead in the polypropylene aerosol membrane
- JSLIST carbon beads

The IPFS configurations are manufactured assemblies of the above layers and are illustrated in **Table 2**. A separate IPFS manufacturing report is in preparation and will go into more detail on the actual configuration fabrication. **Table 2** serves to show the layered structure through which aerosol skin deposition must occur through material penetration. The C4, C5, and C7 concepts are garment-over-garment configurations and are shown as two rows in **Table 2**. Also included in **Table 2** are sub-structures of the complete layered configurations (with "M" and "L" designations) which were characterized by swatch level aerosol testing. The "M" designation generally refers to outer material layers and the "L" designation generally refers to liner material layers.

Table 2. Material layers of garment configurations

Structure	Repellent finish	Shell fabric	Aerosol membrane	Reactive membrane	Sorptive material
C1 & C2	UltraEverShield	Defender M Stretch FR	TX3109		StedCarb
M1	UltraEverShield	Defender M Stretch FR	TX3109		
L1					StedCarb
C3 base	UltraEverShield with 8-HQ/BIT	Sigma Versatech FR		PVAM with 8-HQ/BIT	
M5	UltraEverShield with 8-HQ/BIT	Sigma Versatech FR			
L2				PVAM with 8-HQ/BIT	
C3 vent	UltraEverShield with 8-HQ/BIT	Sigma Versatech FR	TX3114		Zorflex
M6	UltraEverShield with 8-HQ/BIT	Sigma Versatech FR	TX3114		
L3					Zorflex
C4 (EFRACU)	UltraEverShield	Sigma 4 Star	TX3109		
C4 (CBUG)					Saratoga #103774
M2 (EFRACU)	UltraEverShield	Sigma 4 Star	TX3109		
M4 (CBUG)					Saratoga #103774
C5 (CBEC)	UltraEverShield	Cotton/polyester (in Saratoga #101765)	polypropylene (in Saratoga #101765)		carbon beads (in Saratoga #101765)
C5 (FRACU)		Defender M FR			
M3 (CBEC)	UltraEverShield	Cotton/polyester (in Saratoga #101765)	polypropylene (in Saratoga #101765)		carbon beads (in Saratoga #101765)
C6 (JSLIST)	Quarpel	Nylon/cotton			carbon beads
C7 (JSLIST)	Quarpel	Nylon/cotton			carbon beads
C7 (FRACU)		Defender M FR			

2.2 Aerosol Swatch Testing

Aerosol swatch filtration efficiencies of the structures shown in **Table 2** were determined through constant flow rate methods at both NSRDEC and Battelle. Details of the procedures and materials tested at each location are described in the following sections.

2.2.1 NSRDEC Aerosol Swatch Testing

The aerosol filtration efficiency of the IPFS materials was examined by using a TSI Automated Filter Tester Model 3160 that measures particle penetration versus particle size at a set aerosol flow rate (face velocity). TSI 3160 can generate two kinds of aerosol particles in the range of 0.015 to 0.8 μm, polydisperse dioctylphtalate (DOP, oil) or NaCl (salt), using an atomizer. The TSI 3160 is capable of measuring efficiencies up to 99.999999%. Flow rates were set to achieve a sample face velocity of 5.0 cm/s. The 5.0 cm/s face velocity was selected based on Test Operations Procedure (TOP) 08-2-501A (2013). The filtration efficiencies for the samples addressed in this report were reported at a face velocity of approximately 5.4 cm/s (resulting from the 5.0 cm/s set point). Generally, three replicate measurements were averaged for the reported values. While some measurements were made with the salt aerosol challenge, most were made using DOP.

The TSI 3160 is equipped with two TSI Model 3772 Condensation Particle Counters (CPCs). The Model 3772 CPC detects particles as small as 0.010 μm in diameter and employs single-particle-count-mode operation to measure concentrations up to 10,000 particles per cm^3. The detector counts individual pulses produced as each particle (droplet) passes through the sensing zone. A high signal-to-noise ratio and continuous, live-time coincidence correction provides accuracy even at very low concentrations. The Model 3772 CPC uses a laser-diode light source and a diode photodetector to collect scattered light from particles

The TSI 3160 is also equipped with a TSI Model 3302A Diluter to reduce the particle concentration of high-concentration aerosols. The Diluter is calibrated for dilution ratios of 100:1 and 20:1 at a total flow rate of 5 L per min.

2.2.2 Battelle Aerosol Swatch Testing

Aerosol swatch testing was carried out at Battelle (Columbus, OH) and is described in detail in Appendix G of the Battelle report. Aerosol penetration was measured over a range of 0.09 to 2.3 μm, with a measurement made for 0.1 μm as specified in the TTA. The swatches were challenged with a polydisperse aerosol of a low-volatility liquid, polyalphaolefin (PAO). The number concentration and size distribution were characterized using a laser aerosol spectrometer (LAS-XII, TSI, Inc., Shoreview, MN). The aerosol filtration efficiency was determined based on the measured particle number concentrations. Aerosol filtration efficiency is a relative performance measurement and is not time (or concentration) dependent other than how particle loading affects penetration. The objective of this effort was only to measure the initial aerosol filtration efficiency and not the effect of particle loading.

Data were collected at a single test condition (i.e., face velocity of 1.8 cm/s) to compare swatch performance. Limited testing was also performed at a face velocity of 5.0 cm/s for comparison. The 5.0 cm/s face velocity was selected based on TOP 08-2-501A (2013). A control material consisting of a glass fiber filter (GFF) media (e.g., Type A/E, Pall Corporation, Port Washington, NY) was used as a negative control with the purpose of providing a high-efficiency filter to demonstrate that if the suit fabric was highly efficient at removing particles, the test apparatus and method would be able to measure a filtration efficiency of at least 99% (< 1% penetration). The control results were used to demonstrate that any penetration measured through the swatch materials was not attributed to leakage or erroneous system operation.

2.3 Aerosol System Testing

AST was carried out at RTI (Research Triangle Park, NC) and is described in detail in Appendix B of the Battelle report. The aerosol system tests were performed in RTI's wind tunnel exposure room with volunteer subjects wearing the different configurations. The wind tunnel contains a 7-ft diameter, 40-hp vane-axial fan centrally located in a 28-ft by 50-ft sealed room. RTI conducted AST with target test conditions of 10 mph wind speed, an air temperature of 70 °F ± 5 °F, and a relative humidity of 50% ± 10%. The exposure period was 30 min. A 2.5-3.0 μm mass median diameter (MMD) aerosol was generated as a solid-phase aerosol. The target concentration of aerosol during the tests was 167 mg/m^3, which provided a target aerosol concentration multiplied by exposure time (Ct) value of approximately 5,000 mg·min/m^3. The standard aerosol is the solid-phase, fluorescently tagged silica powder, as specified in TOP 10-2-022A (2013). This aerosol has a MMD of approximately 2.8 μm with a size range from approximately 0.2 to 20 μm. The distribution of particles size is shown in **Figure 2**.

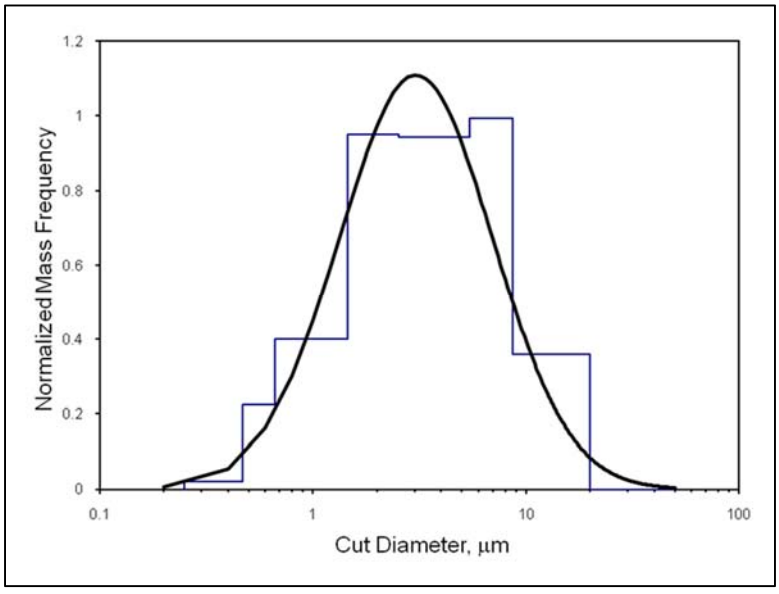

Figure 2. Typical mass distribution of the tagged silica powder aerosol used at RTI for AST

Subjects performed a prescribed motion routine throughout the 30-minute exposure duration. Up to 52 locations on the subjects' skin were sampled through a rinsing procedure after doffing, and a quantitative fluorometric analysis was used on the extract to determine the deposition of the

aerosol (**Figure 3**). Description of the aerosol composition and generation and the detailed donning and doffing procedures for the configurations are included in the Battelle report. Government representatives were on site at RTI for nearly every test to ensure proper and consistent donning and doffing of the garments.

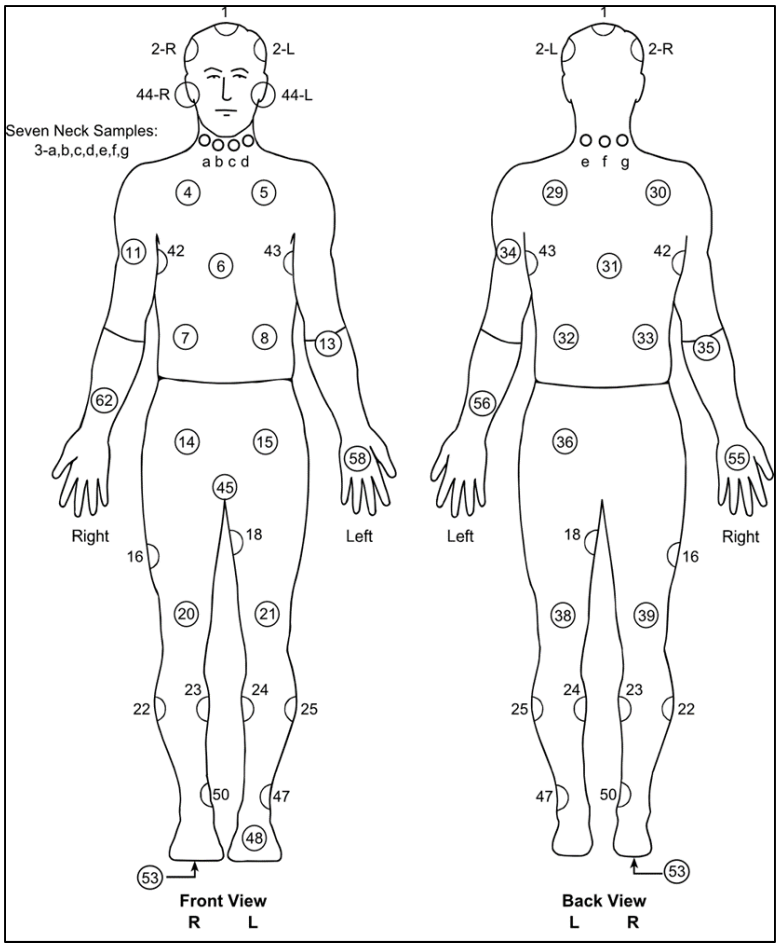

Figure 3. Sampling locations on the skin

AST was carried out on the five IPFS configurations (C1 through C5) and two control configurations (C6 and C7), as shown in **Table 3**. Five replicates of each configuration were tested with a different test participant for each run (out of a pool of six participants). In addition to the configuration described in the first section, the test participants also wore briefs, t-shirt, socks, mask, gloves, boots, Alternative Footwear Solution (AFS) overboots, Improved Outer Tactical Vest (IOTV), and Advanced Combat Helmet (ACH). A photograph of the garment ensemble C1, taken just prior to entering the wind tunnel, is presented in **Figure 4**.

Table 3. Components of the IPFS garment ensembles for AST.

Test Item	AST Configuration Code						
	C1	C2	C3	C4	C5	C6	C7
Boxer briefs	X	X	X	X	X	X	X
T-shirt	X	X	X		X	X	X
Black athletic socks	X	X	X	X	X	X	X
C1 coverall	X						
C2 coat & trousers		X					
C3 coverall			X				
C4 inner pants & shirt				X			
C4 outer coat & trousers				X			
C5 coverall					X		
JSLIST Type II coat & trousers						X	X
FRACU					X		X
M50 mask	X	X	X	X	X	X	X
Mask carrier	X	X	X	X	X	X	X
JB1GU-FR gloves with CB liners	X	X	X	X	X	X	X
Hot weather combat boots	X	X	X	X	X	X	X
AFS overboots	X	X	X	X	X	X	X
IOTV with plates	X	X	X	X	X	X	X
ACH helmet	X	X	X	X	X	X	X

Figure 4. Pre-test photograph of the IPFS garment ensemble C1 with equipment for AST

3. RESULTS AND DISCUSSION

3.1 NSRDEC Aerosol Swatch Testing on New Materials

Table 4 contains the results for filtration efficiency measurements for swatches of the IPFS configurations described in the previous section. **Table 4** corresponds to the fabric structures shown in **Table 2,** including the sub-structures with the "M" and "L" designations. Also shown in **Table 4** are some of the shell fabrics without a laminated aerosol membrane. Swatch level measurements on the aerosol membrane were not carried out due to the mechanical fragility of the membranes as self-standing films. The two rows for C4, C5, and C7 in **Table 2** are combined into one row in **Table 4** to show the overall filtration efficiency of the garment-over-garment configuration that these concepts represent. Since the C3 base material is an air-impermeable material, aerosol measurements were not possible. The solid filled spaces in **Table 4** represent samples that were not measured. All values shown in **Table 4** are for the DOP aerosol permeation.

Table 4. Filtration efficiency for IPFS garment configurations and sub-structures at 5.4 cm/s measured at NSRDEC

Swatch material configuration sub-structure	**Filtration Efficiency at 5.4 cm/s**			
	% @ 0.1 µm	**% @ 0.3 µm**	**% @ 0.5 µm**	**% @ 0.8 µm**
C1 & C2	56	68	63	63
M1	48	62	49	49
L1	17	10	26	26
M1 (w/o TX3109)	9	8	12	13
C3 base	n/a	n/a	n/a	n/a
M5	3	2	5	6
L2	n/a	n/a	n/a	n/a
C3 vent	89	97	90	90
M6	88	97	89	89
L3	10	3	16	16
M6 (w/o TX3114)	3	2	5	6
C4	42	35	52	54
M2	32	30	40	41
M4	16	7	20	21
M2 (w/o TX3109)	6	6	4	5
C5				
M3	70	58	48	49
FRACU				
C6	29	26		
C7				

First, addressing the full garment configuration swatches of C1 through C7, the C3 vent material showed the highest measured swatch filtration efficiency. Only the C3 base is considered even higher due to its air impermeability. The C3 vent material is the only one of the garment configurations to incorporate the StedAir TX3114 aerosol membrane, which is visually the thicker ePTFE membrane when compared to the StedAir TX3109, incorporated into the C1, C2, and C4 configuration materials. All of the membrane-containing materials show a higher filtration efficiency than the C6 control material, which does not contain an aerosol barrier layer.

The "M" designated M1 through M6 sub-structure samples all represent finished shell materials with M1, M2, M3, and M6 containing a laminated aerosol membrane while M4 and M5 do not. Again, the highest swatch filtration efficiency of this group of materials is associated with the only sample containing the thicker TX3114 ePTFE membrane (M6). The M3 sample shows the second highest filtration efficiency, but is a complete fabric system itself consisting of a shell, membrane, and carbon bead layers. The M1 and M2 samples, containing the lighter TX3109 ePTFE membrane, show lower swatch filtration efficiencies than the M6 and M3 samples, but higher than the M4 and M5 samples that contain no aerosol membrane.

The clear impact of the aerosol membrane on the swatch filtration efficiency is shown for the M1, M2, and M6 samples that were tested with and without the laminated aerosol membrane. These are shown in **Table 4** to provide very little resistance to aerosol penetration.

3.2 Battelle Aerosol Swatch Testing on New Materials

As described in the Experimental Section chapter, aerosol swatch filtration efficiency was measured at Battelle at 1.8 and 5.0 cm/s face velocities. Five swatches of each material were tested at 1.8 cm/s and two swatches at 5.0 cm/s. The results for these tests on the IPFS configurations are shown as the averages in **Tables 5 and 6**, respectively. Since the C3 base material is an air-impermeable material, aerosol measurements were not possible. Detailed graphs of the filtration efficiencies as functions of particle size can be seen in the Battelle report.

Table 5. Filtration efficiency for IPFS configurations at 1.8 cm/s measured at Battelle

Swatch material	**Filtration Efficiency at 1.8 cm/s**					
	% @ 0.1 µm	**% @ 0.3 µm**	**% @ 0.5 µm**	**% @ 0.8 µm**	**% @ 1.0 µm**	**% @ 1.8-2.3 µm**
C1 & C2	66	71	80	85	91	95
C3 base	n/a	n/a	n/a	n/a	n/a	n/a
C3 vent	96	99	100	100	100	100
C4	54	52	60	69	74	88
C5	73	73	78	82	87	93
C6	47	36	37	40	46	61
C7	52	43	44	47	53	67

Table 6. Filtration efficiency for IPFS configurations at 5.0 cm/s measured at Battelle

Swatch material	Filtration Efficiency at 5.0 cm/s					
	% @ 0.1 µm	% @ 0.3 µm	% @ 0.5 µm	% @ 0.8 µm	% @ 1.0 µm	% @ 1.8-2.3 µm
C1 & C2	55	69	82	90	93	98
C3 base	n/a	n/a	n/a	n/a	n/a	n/a
C3 vent	88	98	100	100	100	100
C4	45	50	63	74	79	94
C5	56	54	59	67	72	82
C6	32	24	29	39	47	81
C7						

Generally, aerosol filtration efficiencies increased with particle size at both face velocities with some indication of lower efficiencies in the 0.3 to 0.5 µm range for some samples. Generally, aerosol filtration efficiency decreased with increasing face velocity at the lowest particle sizes, but there was less of a difference with face velocity at the larger particle sizes. The C3 vent material showed the highest filtration efficiency at both face velocities. The C6 and C7 materials showed the lowest filtration efficiencies.

3.3 Comparison of Swatch Testing Results

A comparison of the NSRDEC results at 5.4 cm/s (**Table 4**) with the Battelle results at 5.0 cm/s (**Table 6**) is shown in **Table 7**. Very good agreement is observed for the efficiencies at 0.1 µm and, with the exception of the C4 values, at 0.3 µm. While the Battelle results showed increasing filtration efficiencies at the larger aerosol sizes, the NSRDEC results did not show a similar increase. A glass fiber control was used with the Battelle testing to show that their instrument was measuring properly at all aerosol sizes. A control was not used at NSRDEC for this set of samples. The differences observed at the larger particle sizes could be associated with instrumentation differences that use of a control would have helped to detect.

Table 7. Comparison of NSRDEC swatch filtration efficiencies at 5.4 cm/s with Battelle swatch filtration efficiencies at 5.0 cm/s

Swatch material	NSRDEC	Battelle	NSRDEC	Battelle	NSRDEC	Battelle	NSRDEC	Battelle
	% @ 0.1 µm		% @ 0.3 µm		% @ 0.5 µm		% @ 0.8 µm	
C1 & C2	56	55	68	69	63	82	63	90
C3 base	n/a	n/a	n/a	n/a	n/a	n/a	n/a	n/a
C3 vent	89	88	97	98	90	100	90	100
C4	42	45	35	50	52	63	54	74
C5		56		54		59		67
C6	29	32	26	24		29		39
C7								

A limited amount of measurements were made of the pressure required to maintain the face velocity in the aerosol swatch tests at both NSRDEC and Battelle. These are presented in **Table 8** for the 0.1 µm data at 1.8 cm/s at Battelle and at 5.4 cm/s at NSRDEC. The pressure

drop measured at NSRDEC is higher at the higher face velocity (as expected) when compared to the Battelle measured pressure drops. Both sets of swatch data generally show that better filtration efficiency was achieved with the IPFS configurations with a lower pressure drop when compared to the control configurations. In particular, the C5 configuration in the Battelle measurements showed a pressure drop of only 0.06 inches H_2O for an efficiency of 73%. These limited results have implications for achieving aerosol protection with a garment that is also thermally more comfortable and should be further explored.

Table 8. Aerosol filtration efficiency and pressure drop measured for aerosol swatch testing at 0.1 µm

	Filtration Efficiency for 0.1 µm			
Face Velocity	**Battelle 1.8 cm/s**		**NSRDEC 5.4 cm/s**	
Swatch Material	Filtration Efficiency (%)	Pressure Drop (inches H_2O)	Filtration Efficiency (%)	Pressure Drop (inches H_2O)
C1 & C2	66	0.13	56	0.33
C3 base				
C3 vent	93	0.42	89	1.16
C4	54	0.26	42	0.53
C5	73	0.06		
C6	47	0.34	29	1.06
C7	52	0.37		

3.4 NSRDEC Aerosol Swatch Testing on Laundered Materials

Aerosol swatch testing was carried out at NSRDEC on samples M1 through M6 both as new materials and after one laundering cycle (AATCC 135). The swatch aerosol filtration efficiencies before and after washing are shown in **Table 9**. As previously discussed, samples M1, M2, M3, and M6 all contain an aerosol membrane layer. Samples M1 and M2 contain the lighter weight TX3109 ePTFE membrane. Sample M3 has an incorporated PP aerosol layer as part of the fabric system. Sample M6 contains the heavier weight TX3114 ePTFE membrane. Samples M4 and M5 do not contain an aerosol membrane layer; M4 is a separate sorptive layer and M5 is a finished shell material (see Table 2).

Laundering clearly decreased the swatch filtration efficiency of the laminates that contained an incorporated aerosol membrane while the other samples remained essentially the same after laundering. Laundering was observed to initiate delamination of the ePTFE layer with some of the after-laundering filtration efficiencies dropping into the observed single layer values. The M6, with the heavier ePTFE layer, retained more of its filtration efficiency than the M1 and M2 samples, which contained the lighter ePTFE layer. The fabric system M3 sample, containing the PP aerosol layer as part of its fabric system, retained similar efficiencies after laundering (on the average) when compared to the heavier ePTFE results for the M6 sample.

Table 9. Filtration efficiency for IPFS layer combinations both new and after one laundering

Swatch material	Filtration Efficiency at 5.4 cm/s			
	% @ 0.1 µm	% @ 0.3 µm	% @ 0.5 µm	% @ 0.8 µm
M1	48	62	49	49
M1 laundered	15	10	22	22
M2	32	30	43	43
M2 laundered	19	19	26	26
M3	70	58	48	49
M3 laundered	50	32	43	43
M4	13	2	20	21
M4 laundered	13	5	22	22
M5	2	1	5	6
M5 laundered	4	11	9	8
M6	88	97	89	89
M6 laundered	72	85	72	72

3.5 Aerosol System Testing

3.5.1 Aerosol Deposition

The skin rinse method used for AST described in the Experimental Section chapter yields a measure of aerosol deposition velocity (DV) for each of the body regions measured. The DV as a function of body region is shown in **Figure 5** for all the IPFS configurations. The body regions shown represent combinations of the individual locations of the skin rinsed areas. Each point is the geometric mean deposition from the five replicate runs for the particular configuration. More detail is available in Appendix B of the Battelle report.

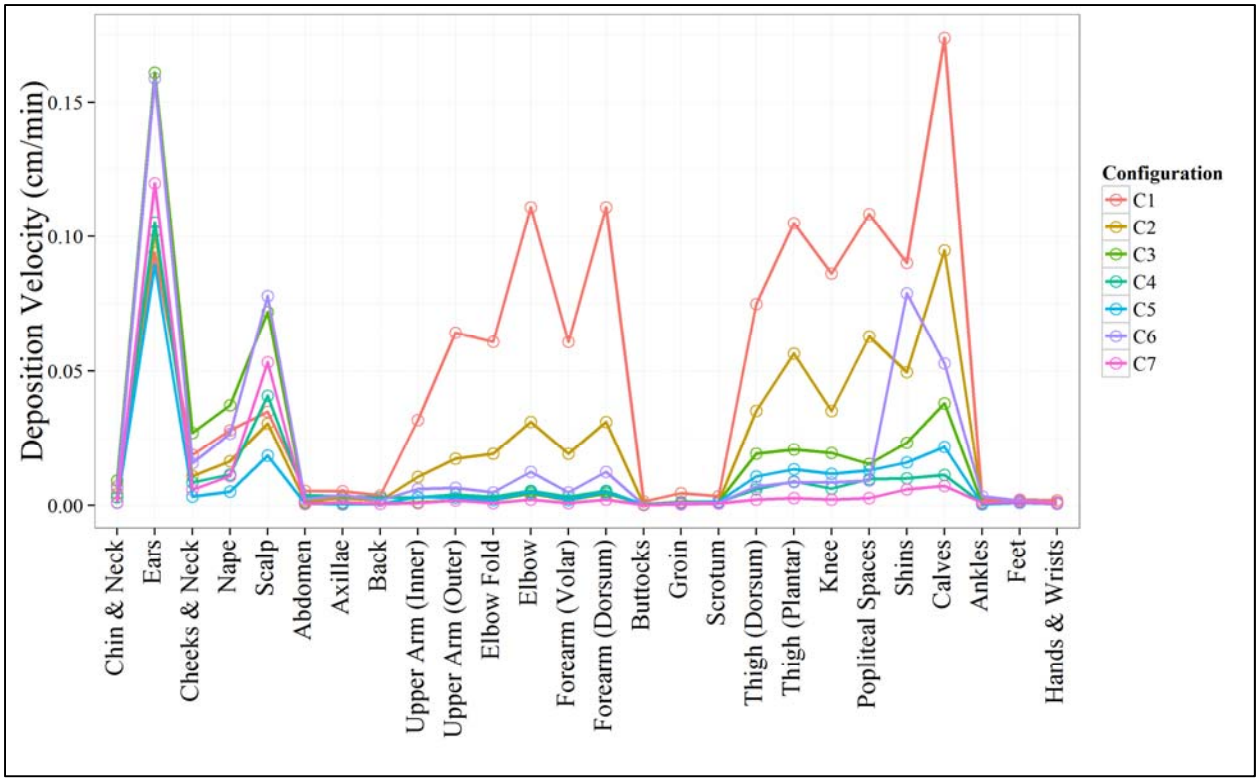

Figure 5. Graphical representation of geometric mean DVs for selected body regions for the IPFS ensembles

3.5.2 Body Region Hazard Analysis from Whole Configuration

The Body Region Hazard Analysis (BRHA) is a model that measures the performance of protective ensembles against percutaneous threats for configurations tested in both the vapor and aerosol system testing (see TOP 10-2-022A). The input for aerosol is the DV values shown in **Figure 5**. The BRHA model examines both local and whole-body systemic health effects, and a 50% cytotoxicity value (CT_{50}) is computed, as defined below, for each case. When interpreting BRHA results, higher numbers mean the configuration provides better protection.

Updated weighting factors (Kierzewski et al., 2011) were used in the local agent calculation based on a recent toxicological study designed to update the BRHA. These updated values correspond to the local body area sensitivities to distilled sulfur mustard (HD) for hot and humid conditions and replace the estimate based on the ratio of body area sensitivities to the chemical nerve agent VX. The new weightings only affect the local results and not the systemic results.

To evaluate for localized effects (for exposure to HD), the weighting factor specified in the BRHA was divided by the DV at each body area. This calculation produces a localized exposure dosage (LED) for each body region that represents the highest aerosolized HD agent challenge to which each body region could be externally exposed before the onset of burns and blisters in 50 percent of the population. The resulting LED values were compared with each other, and the lowest value was selected as the suit performance value. This minimum value is the overall local minimum exposure dosage (MED_{HD}). The MED_{HD} value compares all of the body regions and

chooses the region that is most susceptible to the outside challenge based on the protection in the region and the sensitivity of the region to agent. This means that the most susceptible region may not necessarily be the region with the most breakthrough. It could be a region that had less breakthrough but is more sensitive to agent. Typically, the most susceptible regions are in the head/mask/suit interface or the crotch/groin region.

To evaluate for systemic effects, the DV at each body area was multiplied by the systemic weighting factor provided by the BRHA. The resulting values were summed over all of the body areas and divided into a constant provided by the BRHA to calculate the overall systemic agent minimum exposure dosage (MED_{SYS}). The MED_{SYS} represents the highest aerosolized nerve agent challenge to which the ensemble could be externally exposed before the onset of nausea and vomiting in 50 percent of the population. The MED_{SYS} value uses the body region sensitivities and the body regions area to calculate the ability of the configuration to protect against systemic agents. This value can be thought of as a type of weighted average of performance over the entire body.

Calculated MED_{SYS} and MED_{HD} values for all AST runs for the IPFS configurations, including the test participant, are shown in **Tables 10 and 11**, respectively.

Table 10. Calculated MED_{SYS} values for the IPFS AST configurations

Test Participant	AST Configuration						
	C1	C2	C3	C4	C5	C6	C7
	MED_{SYS}	MED_{SYS}	MED_{SYS}	MED_{SYS}	MED_{SYS}	MED_{SYS}	MED_{SYS}
4	6,959	4,910	10,254	7,611	13,327	11,250	14,022
5	2,271	3,362	4,606	12,019	7,530	2,682	6,348
7		13,946	13,154		26,854	8,539	38,332
13	2,024			9,668			
15	3,358	7,023	9,779	18,758	14,734	6,484	9,604
17	4,254	6,098	7,469	16,609	40,231	11,749	51,234

Table 11. Calculated MED_{HD} values for the IPFS AST configurations

Test Participant	AST Configuration						
	C1	C2	C3	C4	C5	C6	C7
	MED_{HD}	MED_{HD}	MED_{HD}	MED_{HD}	MED_{HD}	MED_{HD}	MED_{HD}
4	223,900	55,702	122,198	66,158	132,820	165,194	81,783
5	101,438	72,283	57,004	90,565	125,130	44,521	59,401
7		353,582	92,658		264,527	106,034	284,321
13	113,171			68,498			
15	29,389	49,050	31,595	73,211	51,565	17,708	20,658
17	182,863	267,313	144,793	189,038	172,257	274,327	644,767

The results presented in **Tables 10 and 11** show that significant scatter is observed in the calculated MED values for the five replicate runs of each configuration. Since one of the goals of the program is to determine whether differences in aerosol system performance between the configurations exist, statistical analysis of this scatter was necessary. The TOP 10-2-022A

specifies the use of a geometric mean to present the deposition and BRHA data. A simple geometric mean of the MED values for each configuration was calculated along with the low and high values for the 95% confidence interval. Since AST used six participants to run five replicates (see the "blanks" for test participants 7 and 13 in **Tables 10 and 11**), the use of the least squares (LS) geometric mean should provide a more accurate representation of this "unbalanced" data set. LS geometric means and their corresponding low and high values for the 95% confidence intervals were calculated at NSRDEC using the SAS software package; at RTI using the R software package; and at Battelle using the R software package. All of the calculated means and their corresponding low/high values are shown in **Table 12** for the MED_{SYS} values from **Table 10** and shown in **Table 13** for the MED_{HD} values in **Table 11**.

Table 12. Geometric means for MED_{SYS} data with 95% confidence intervals

Configuration	Analysis	MED_{SYS}		
		95% high	**mean**	**95% low**
C1	geometric	6,323	3,404	1,832
	LS geometric NSRDEC	6,396	3,766	2,217
	LS geometric RTI	6,544	3,766	2,167
	LS geometric Battelle	6,642	3,862	2,245
C2	geometric	12,067	6,292	3,280
	LS geometric NSRDEC	10,026	5,880	3,449
	LS geometric RTI	10,288	5,880	3,361
	LS geometric Battelle	9,955	5,774	3,349
C3	geometric	14,016	8,538	5,201
	LS geometric NSRDEC	13,606	7,980	4,680
	LS geometric RTI	13,962	7,980	4,561
	LS geometric Battelle	13,509	7,835	4,544
C4	geometric	19,465	12,247	7,706
	LS geometric NSRDEC	23,013	13,549	7,978
	LS geometric RTI	23,545	13,549	7,797
	LS geometric Battelle	23,898	13,895	8,078
C5	geometric	39,017	17,405	7,764
	LS geometric NSRDEC	27,736	16,267	9,540
	LS geometric RTI	28,462	16,267	9,297
	LS geometric Battelle	27,539	15,973	9,264
C6	geometric	15,264	7,221	3,416
	LS geometric NSRDEC	11,507	6,749	3,958
	LS geometric RTI	11,808	6,748	3,857
	LS geometric Battelle	11,425	6,626	3,843
C7	geometric	53,419	17,579	5,785
	LS geometric NSRDEC	28,012	16,429	9,635
	LS geometric RTI	28,747	16,430	9,390
	LS geometric Battelle	27,815	16,132	9,357

Table 13. Geometric means for MED_{HD} data with 95% confidence intervals

Configuration	Analysis	MED_{HD}		
		95% high	**mean**	**95% low**
C1	geometric	285,100	106,674	39,914
	LS geometric NSRDEC	253,869	120,415	57,115
	LS geometric RTI	267,322	120,419	54,244
	LS geometric Battelle	263,504	128,198	62,369
C2	Geometric	358,213	113,295	35,833
	LS geometric NSRDEC	231,733	109,371	51,620
	LS geometric RTI	244,571	109,367	48,907
	LS geometric Battelle	238,944	115,870	56,188
C3	Geometric	168,797	78,351	36,368
	LS geometric NSRDEC	160,258	75,637	35,698
	LS geometric RTI	169,136	75,634	33,822
	LS geometric Battelle	165,246	80,132	38,858
C4	Geometric	153,551	89,304	51,938
	LS geometric NSRDEC	212,538	100,811	47,816
	LS geometric RTI	223,791	100,810	45,411
	LS geometric Battelle	220,595	107,322	52,213
C5	Geometric	276,607	131,318	62,343
	LS geometric NSRDEC	268,590	126,766	59,830
	LS geometric RTI	283,477	126,765	56,687
	LS geometric Battelle	276,955	134,303	65,127
C6	Geometric	317,998	82,355	21,328
	LS geometric NSRDEC	168,441	79,499	37,521
	LS geometric RTI	177,779	79,499	35,551
	LS geometric Battelle	173,690	84,227	40,844
C7	Geometric	603,689	112,967	21,139
	LS geometric NSRDEC	231,062	109,054	51,470
	LS geometric RTI	243,862	109,050	48,765
	LS geometric Battelle	238,252	115,534	56,025

Tables 12 and 13 serve to show the importance of both using the LS geometric means and the selection of the data set used to calculate the LS geometric means. The simple geometric means and the LS geometric means calculated at NSRDEC and RTI use the values shown in **Tables 10 and 11** for C1 through C7 as the data set. If the data sets were balanced (no "blanks"), the simple and LS geometric means would be identical. Since the data set is unbalanced (the five replicate ASTs for each configuration utilized six different test participants) differences between the simple geometric mean and the LS geometric mean from the NSRDEC and RTI analysis are observed. While the calculated LS geometric means from the NSRDEC and RTI analyses are in good agreement, the two different software packages used yielded slightly different confidence

intervals. The R software used at RTI yielded a somewhat broader confidence interval at 95% (lower lows and higher highs) when compared to the interval calculated with the SAS software used at NSRDEC.

Also included in **Tables 12 and 13** are the LS geometric means calculated at Battelle. The data set used in this analysis included an additional configuration (a total of eight configurations) that was part of the RTI report in Appendix B of the Battelle report, but not part of the IPFS study. It can be seen in **Tables 12 and 13** that the inclusion of this additional configuration in the data set affected the values for the LS geometric mean and the 95% confidence interval calculated for all the other configurations. This observation points out the importance of specifying the considered data set for the calculation of means and confidence intervals of unbalanced data sets to be compared for statistically significant differences between configurations. Further comparisons in this report will focus only on the results from the NSRDEC and RTI LS geometric mean calculations for the data set specified in the particular analysis discussed.

A chart of the NSRDEC SAS results for the LS geometric means and the corresponding 95% confidence intervals for each IPFS configuration from **Table 12** are shown in **Figure 6** for the MED_{SYS} data and from **Table 13** are shown in **Figure 7** for the MED_{HD} data. Also shown in **Figures 6 and 7** are lines indicating the LS geometric mean, the 95% high, and 95% low for the C6 configuration, which represents the CB control configuration and is used in further comparison discussion.

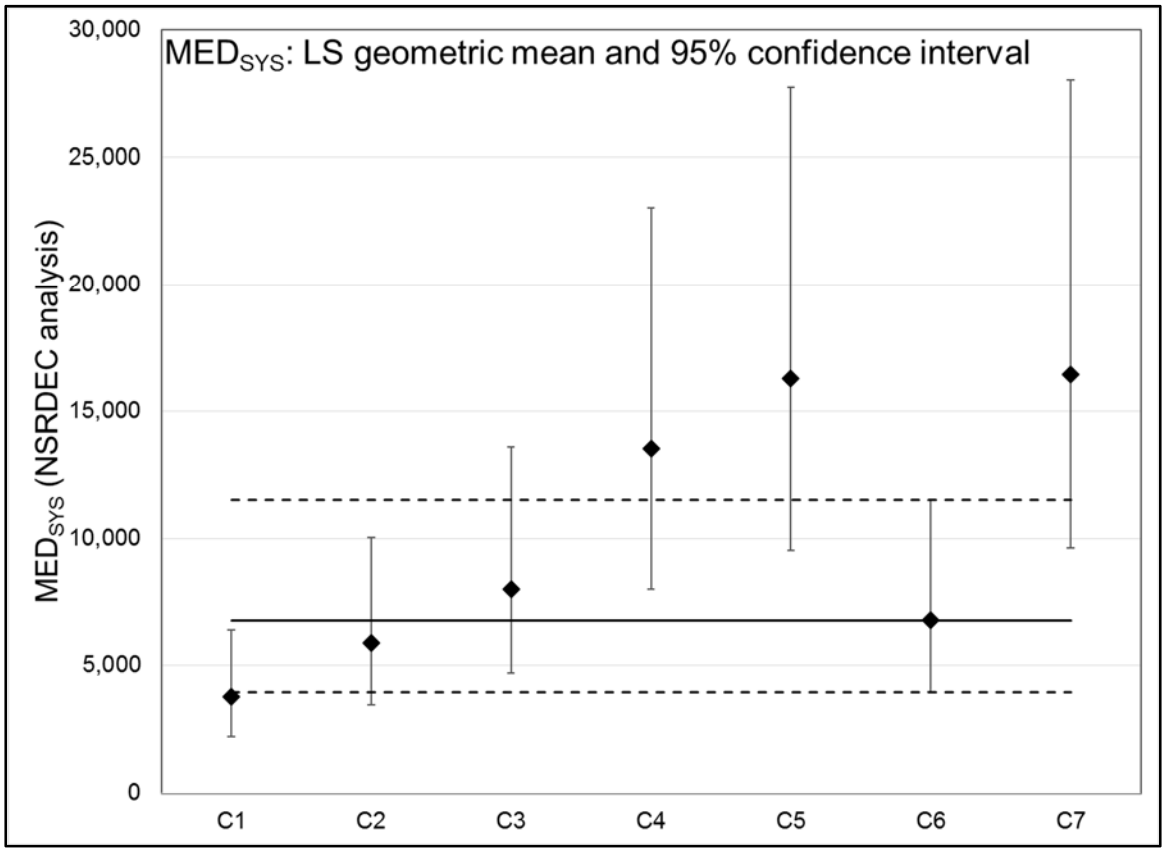

Figure 6. LS geometric mean of MED_{SYS} data from AST and 95% confidence interval

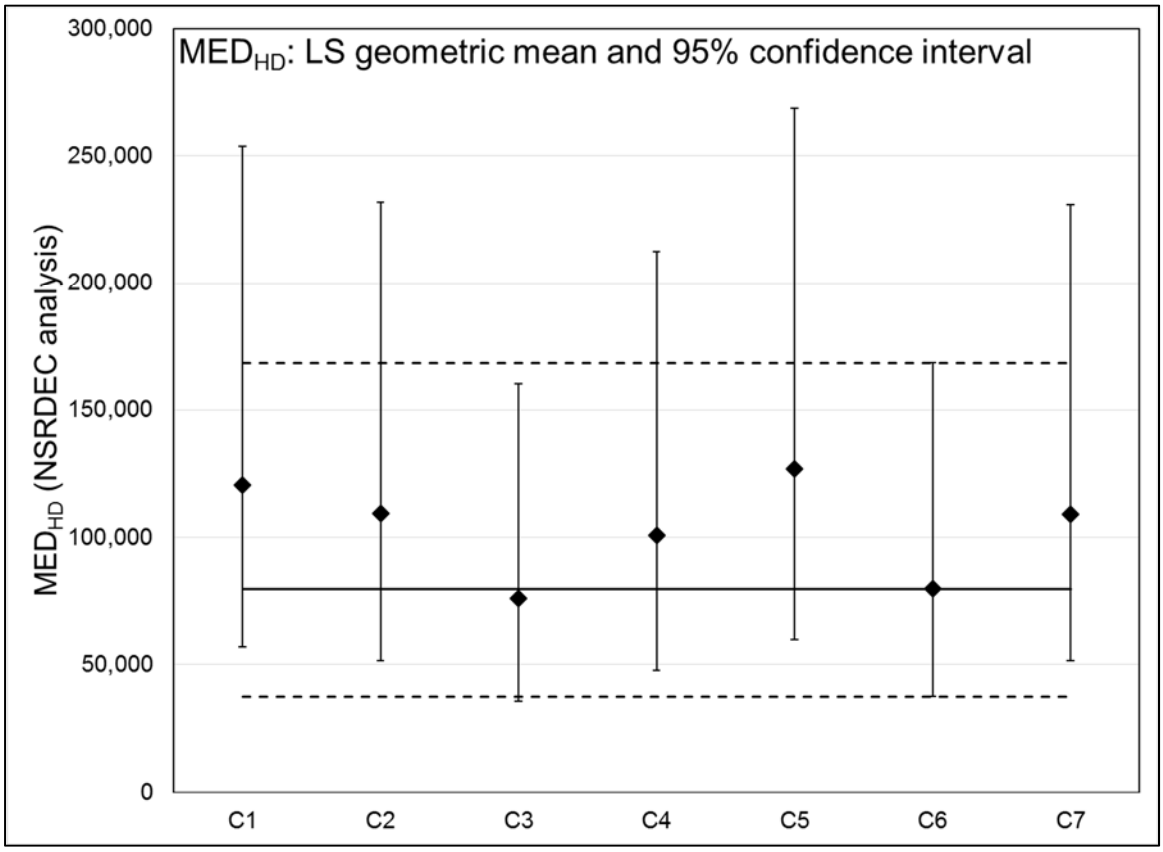

Figure 7. LS geometric mean of MED_{HD} data from AST and 95% confidence interval

At the simplest level, the LS geometric mean for MED_{SYS} of C3, C4, C5, and C7 are higher (better) than C6 while C1 and C2 are lower than C6. The LS geometric mean for MED_{HD} of C1, C2, C4, C5, and C7 are higher (better) and only C3 is lower (slightly) than C6. However, because of the significant scatter observed in the aerosol deposition for the replicate AST runs of the same configuration, the statistical significance of the differences in the means needs to be addressed.

The overall goal of the BRHA analysis for the IPFS ensembles was to compare the derived values for the performance of the candidate ensembles with a CB control. A discussion of the statistically significant differences based on the BRHA comparing the IPFS configurations C1 through C5 to the CB control configurations C6 and C7 are presented in Appendix B of the Battelle report. Comparisons were made at RTI using analysis of variance (ANOVA) techniques. The comparison of the ensemble performance involved Dunnett's test for multiple comparisons against a reference. Each of the IPFS ensembles (C1 through C5) was compared to either the C6 configuration or the C7 configuration. The C6 comparisons did not include the C7 data and the C7 comparisons did not include the C6 data.

Table 14 summarizes the results of these comparison tests for the IPFS ensembles. The key parameter presented in this analysis is the p-value column in the table. If this value is less than

0.05, then that particular comparison is statistically different at the 95% confidence level (α=0.05). For nerve agents (systemic effect MED_{SYS}), the C4 and C5 ensembles performed statistically better and the C1 ensemble statistically worse than the C6 baseline with the differences of C2 and C3 to C6 not statistically different at the 95% level. When compared to the C7 baseline the C1, C2, and C3 ensembles performed statistically worse than the C7 baseline with C4 and C5 not statistically different at the 95% level. For blistering agents (local effect MED_{HD}), no statistically significant differences were found in the protection capability of any of the five ensembles in the IPFS test matrix when compared with either the C6 baseline or the C7 baseline.

Table 14. Summary of the IPFS test series ensembles compared to the C6 and C7 configurations

Measure	Comparison	Estimate	p-value	Significant difference at 95%?	Better or worse than C6?
Comparison to C6					
MED_{SYS}	C1 to C6	-0.6038	0.048	Yes	Worse
	C2 to C6	-0.1377	0.966	No	n/a
	C3 to C6	0.1676	0.925	No	n/a
	C4 to C6	0.6770	0.020	Yes	Better
	C5 to C6	0.8798	<0.001	Yes	Better
MED_{HD}	C1 to C6	0.3941	0.557	No	n/a
	C2 to C6	0.3190	0.771	No	n/a
	C3 to C6	-0.0498	1.000	No	n/a
	C4 to C6	0.2163	0.928	No	n/a
	C5 to C6	0.4666	0.359	No	n/a
Comparison to C7					
MED_{SYS}	C1 to C7	-1.4615	<0.001	Yes	Worse
	C2 to C7	-1.0275	<0.001	Yes	Worse
	C3 to C7	-0.7222	0.023	Yes	Worse
	C4 to C7	-0.1811	0.941	No	n/a
	C5 to C7	-0.0100	1.000	No	n/a
MED_{HD}	C1 to C7	0.1145	0.997	No	n/a
	C2 to C7	0.0029	1.000	No	n/a
	C3 to C7	-0.3659	0.655	No	n/a
	C4 to C7	-0.0633	1.000	No	n/a
	C5 to C7	0.1505	0.986	No	n/a

Note: *p*-values less than 0.05 indicate a significant difference at the 95% confidence level

Table 15 serves to illustrate the importance of the data set considered to make comparisons through such an analysis. While **Table 14** shows either the data set of C1 through C5 and C6 or the data set of C1 through C5 and C7, **Table 15** shows the results from the ANOVA analysis for the data set of C1 through C5 and both C6 and C7. This changes the derived p-value enough in the C1 comparison with C6 that it is no longer statistically significant at the 95% level as shown in **Table 14**. **Table 15** also shows that C7 is statistically better than C6, a comparison not made with the data sets used in **Table 14**.

Table 15. Comparison of IPFS configurations with C6 when C7 data are included in the calculations

Measure	Comparison	Estimate	p-value	Significant difference at 95%?	Better or worse than C6?
Comparison to C6					
MED_{SYS}	C1 to C6	-0.5834	0.117	No	n/a
	C2 to C6	-0.1377	0.988	No	n/a
	C3 to C6	0.1676	0.969	No	n/a
	C4 to C6	0.6970	0.039	Yes	Better
	C5 to C6	0.8798	0.003	Yes	Better
	C7 to C6	0.8898	0.003	Yes	Better

One additional ANOVA comparison was made with the C2 garment configuration as the point of comparison. The values derived for the MED_{SYS} data for configurations C1 through C6 from this analysis are shown in **Table 16**. Generally, the C2 MED_{SYS} values were similar to the C6 values, as can be seen graphically in **Figure 6**, and both C4 and C5 are statistically better than C2 at the 95% confidence level, similar to the comparisons shown for C6 in **Table 14**. However, while the estimate and fairly low p-value indicate the C1 garment configuration is worse than C2, it is not statistically different at the 95% confidence level. Configurations C1 and C2 are constructed with the same materials, but represent the differences between a one-piece design (C1) and a two-piece design (C2).

Table 16. Comparison of the IPFS configurations with C2 when C1 through C6 data are included in the calculations

Measure	Comparison	Estimate	p-value	Significant difference at 95%?	Better or worse than C2?
Comparison to C2					
MED_{SYS}	C1 to C2	-0.4661	0.187	No	n/a
	C3 to C2	0.3053	0.548	No	n/a
	C4 to C2	0.8143	0.003	Yes	Better
	C5 to C2	1.0175	<0.001	Yes	Better
	C6 to C2	0.1377	0.966	No	n/a

Summarizing this first level of analysis of the BRHA derived MED_{SYS} and MED_{HD} values, the IPFS configurations C1 through C5 only showed statistically significant differences at the 95% confidence level with the CB control baselines for the MED_{SYS} values. The MED_{HD} values effectively reflect only the region of greatest penetration/deposition, with the hood/head region aerosol deposition dominating these values, masking any differences attributed to the ensemble design. The significant differences in the MED_{SYS} values primarily showed the two-layer designs, IPFS configurations C4 and C5, to be better than the C6 baseline, but not significantly different when compared to the two-layer C7 baseline. Further analysis of the statistical variation was carried out through modeling efforts at RTI and NSRDEC and is covered in the next sections.

3.5.3 Statistical Modeling Efforts

Since different test participants were used to carry out the replicate AST runs, modeling efforts were carried out at RTI and NSRDEC to determine the level of contribution to the observed variation that could be associated with the different test participant versus the different garment configuration. These efforts are described in the next two sections.

3.5.3.1 RTI modeling

The statistical model used for the above ANOVA was a linear mixed effects model. It was mixed in the sense that it had both fixed and random effects. The fixed effects in this case were the garment configurations. The random effects were the test participants (they were a 'random' sample from a large population of potential test participants). It was possible to use a simpler model accounting for just the fixed effects, but the use of the mixed effects model allowed for splitting out the variability due to the test participants from the variability due to other unaccounted for residual effects. This helped to provide a more sensitive test.

In the mixed effects model used in this analysis, the test participant and residuals had separate contributions to the variance. In the simpler fixed effects model, these values would have been lumped together. This was important because the residual variance was used as the denominator when calculating the *F*-statistic for determining the significance of the configuration fixed effect. The smaller the residual variance, the stronger the configuration effect. So, by using the mixed effects model and separating out the test participant variance, the calculation of the *F*-statistic was improved. The mean square error value for the test participant effect divided by the residual variance gave the *F*-statistic.

For the MED_{SYS}, the garment configuration contributed to 47% of the variability. The test participants and other random effects accounted for the rest of the variability. For the MED_{HD}, the garment configuration contributed to 5% of the variability.

3.5.3.2 NSRDEC modeling

To assess the effects of configuration and test participant on MED_{SYS} and MED_{HD}, three models were created and compared. The configuration was considered the variable of interest and was kept as a fixed effect in each model. Model 1 used only the configuration as a fixed effect. Model 2 used the configuration as a fixed effect and the test participant as a random effect, separating the contributions of the test participant and residual to the variability of MED (effectively the model used by RTI, as described above). Model 3 used both the configuration and test participant as fixed effects, using both variables to explain the variance in MED.

It was found that Model 3 was significantly better than the other models for both MED_{SYS} and MED_{HD}, even though it used more degrees of freedom by fixing both configuration and test participant. For MED_{SYS}, Model 3 shows that 82% of the total variance can be explained with the configuration explaining 52% and the test participant explaining 36%. The variance that each variable explains does not necessarily add up to the total explained variance due to collinearity. Both configuration and test participant had a statistically significant effect on MED_{SYS}. For

MED_{HD}, Model 3 shows that 74% of the total variance can be explained with the configuration explaining 5% and the test participant explaining 69%. While the test participant effect was statistically significant on MED_{HD}, the configuration was not. Model 2 showed only 5% of the variability in MED_{HD} could be explained by the configuration, consistent with the similar model employed by RTI.

3.5.4 Battelle Statistical Analysis

In addition to the RTI statistical analysis of their data in Appendix B of the Battelle report and the NSRDEC analysis of the same data, Battelle provided a supplemental analysis of the RTI AST data and presents it in Appendix C of the Battelle report. Appendix C contains the Battelle analyses of DV and the BRHA analysis outputs. However, the discussion presented in Appendix C is based on the data set that includes the seven configurations associated with the IPFS study along with an additional configuration included from a different study in the RTI report (Appendix B of the Battelle report). As seen in **Tables 12 and 13**, somewhat different means and confidence intervals were derived for this data set, so the statistical significance may be different than that derived from a data set that only included the IPFS configurations.

A sample of the DV analysis in Appendix C of the Battelle report is shown in **Figure 8**. This figure graphically illustrates the statistically (95% confidence) better, same, or worse DVs for the different body regions when C1 is compared to C6. Similar figures are available in Appendix C for all the configuration comparisons and also for the comparisons of the BRHA results from the DVs.

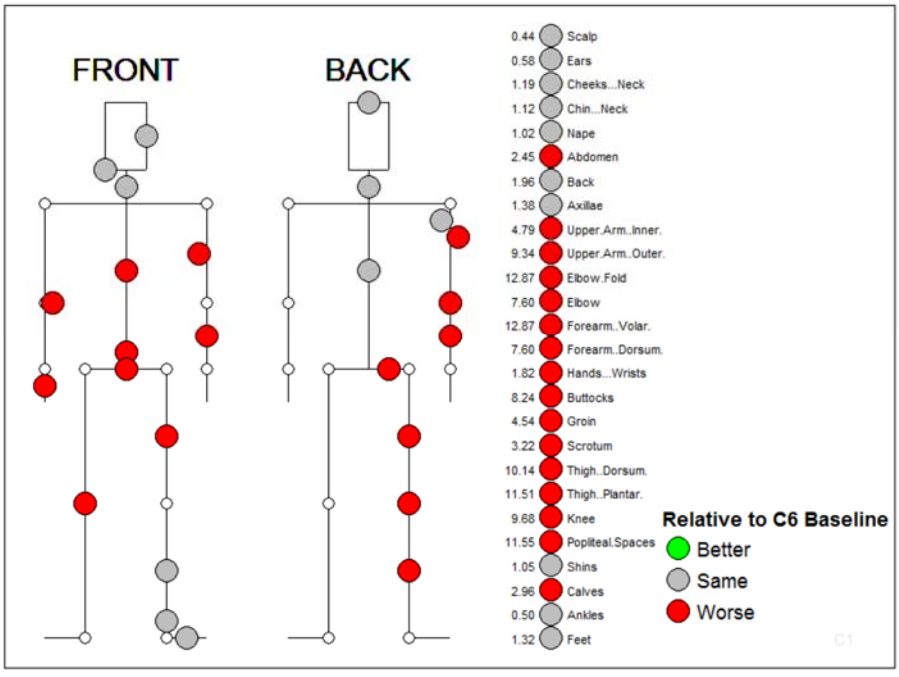

Figure 8. AST DV Results – Ratio of C1 to C6

Also included in Appendix C of the Battelle report are tables like the example shown in **Table 17** for the overall systemic BRHA (MED_{SYS}) for all the configurations. Based on the 95% statistical confidence interval, boxes are drawn around the configurations that are statistically indistinguishable and associated with a "Group" listed in the right-most column of the table. Similar tables are also included in Appendix C of the Battelle report for DV by body region and separate body region derived BRHA values. Configuration B in **Table 17** is the additional garment configuration (not in the IPFS study) included in the data set analyzed by Battelle in their statistical analysis presented in Appendix C of the Battelle report.

Table 17. Systemic Agent Toxicity Index from Appendix C in Battelle report

Configuration	Geometric mean	Lower 95% CI	Upper 95% CI	C7	C5	C4	C3	C6	C2	C1	B	Group
C7	16,132	9,357	27,815		=	=	>	>	>	>	>	A
C5	15,973	9,264	27,539	=		=	>	>	>	>	>	A
C4	13,895	8,078	23,898	=	=		>	>	>	>	>	A
C3	7,835	4,544	13,509	<	<	<		=	=	>	>	B
C6	6,626	3,843	11,425	<	<	<	=		=	>	>	B
C2	5,774	3,349	9,955	<	<	<	=	=		=	>	BC
C1	3,862	2,245	6,642	<	<	<	<	<	=		>	C
B	2,329	1,388	3,907	<	<	<	<	<	<	<		D

Inclusion of this additional configuration may not change the general order and significance of the IPFS configurations, but direct comparisons with the results discussed earlier, based on a data set which does not include this configuration, may not be correct. **Table 17** does show configuration C6 in Group B which is statistically lower than Group A (C4 and C5) and higher than Group C (C1). In earlier discussions based on the RTI analysis of the data set consisting of configurations C1 through C6 (**Table 14**), configuration C1 was considered statistically worse and garment configurations C4 and C5 were considered statistically better than configuration C6, similar to the results shown by Battelle in **Table 17**. In this case, the same statistical differences were observed for the different data sets. Similar to the previous overall observations, the Battelle analysis in **Table 17** shows the two layer configurations (C4, C5, and C7) to be significantly better than the one layer configurations for MED_{SYS}. Also similar, no statistically significant differences between configurations were observed for MED_{HD}.

3.5.5 Mask Sizing

It was noted by RTI that the hood-mask interface is an area of concern when wearing the M50 mask that was part of the overall configuration for AST of all the IPFS ensembles. Black light examinations of the test participants after AST showed bright but localized aerosol deposits near the sideburns for nearly all the tests of the IPFS configurations. These black light photos are included in Appendix B of the Battelle report and one example is shown here in **Figure 9**. It is primarily this region that dominated the calculation of the MED_{HD} values for which statistical analysis, to this point, showed no significant differences between the configurations. RTI also notes that an obvious way to increase the performance of the IPFS ensembles would be to solve the M50 hood-mask leakage issue.

Figure 9. Black light photograph showing localized facial aerosol deposits after AST

In order to address the deposition issues associated with the hood/mask interface region, an attempt was made to relate the facial measurements of each test participant with the size of mask they wore to see if some relationship between fit and performance could be revealed. Anthropometric measurements for each of the six test participants were used. Facial measurements that were not collected were imputed. A statistical model was used to determine the relationship between the mask size and relative facial measurements (linear proportional scaling) to the amount of protection that was provided (natural log of MED_{HD}). It was found that mask size was significant in determining protection ($p = 0.0001$), but the size of the individual's face was not significant ($p = 0.5412$).

A 1988 technical report titled "Sizing Determination Final Report" from the Chemical Research, Development and Engineering Center indicated that facial measurements are actually a poor determiner of mask size (Jackson et al., 1988). Given this information and the fact that facial measurement values needed to be imputed (which are poorly correlated with other body measurements), it was decided to remove the mask bias by recalculating the MED_{HD} values without head measurements.

3.5.6 Below the Neck Analysis of the AST Results

Another approach to addressing the hood/mask region and its deposition impact on the BRHA analysis was to eliminate the head and neck regions from the calculation of MED_{SYS} and MED_{HD} and statistically compare these values for statistically significant differences between the garment configurations. These efforts are described in the next two sections.

3.5.6.1 RTI below the neck analysis

The BRHA analysis was completed for all below the neck body regions for the IPFS configurations C1 through C5 plus the C6 baseline by RTI. The full BRHA has twenty-three body regions, the first five of which cover the neck and head. These five five (Chin & Neck, Ears, Cheeks & Neck, Nape, and Scalp) were removed from the data set, leaving eighteen body

eighteen regions. These five regions are the five left-most points in **Figure 5**, which numerically show the high aerosol depositions from the skin rinse sampling in these regions.

Beginning with the DVs from each test and for each of the eighteen 18 body regions, the LEDs were calculated using the BRHA local toxicity values. The LED values for each test were examined and the lowest value for each test was selected as the MED_{HD} for that test. The systemic contribution from each body region was calculated by taking the DV for each body region, multiplying by the area for that body region, and dividing by the systemic toxicity value for that region. The contributions from each region were then summed and inverted, giving the MED_{SYS} for the test. The LS geometric means and confidence intervals for the averages over each configuration were then calculated.

Shown in **Figure 10** are the MED_{SYS} LS geometric means and 95% confidence intervals for the complete set of twenty-three body regions (solid markers on the left side) and for the eighteen body regions representing the below the neck regions (open markers on the right side). Shown in **Figure 11** are the corresponding data for MED_{HD}. Both **Figures 10 and 11** show the geometric mean and 95% confidence intervals for the C6 configuration as lines for both the full and below the neck body region calculations. The data on the left side of both figures is similar to the corresponding charts shown in **Figures 6 and 7** where C7 was included in the calculations of the LS geometric mean and confidence intervals. Only the C1 through C6 data are used for the calculations illustrated on the right side of **Figures 10 and 11** for the below the neck calculations. Both the calculated MED_{SYS} and MED_{HD} are higher, as expected, since the regions of observable high aerosol deposition were eliminated from the calculations. The greater impact of the below the neck analysis on MED_{HD} is clearly observed in **Figure 11**.

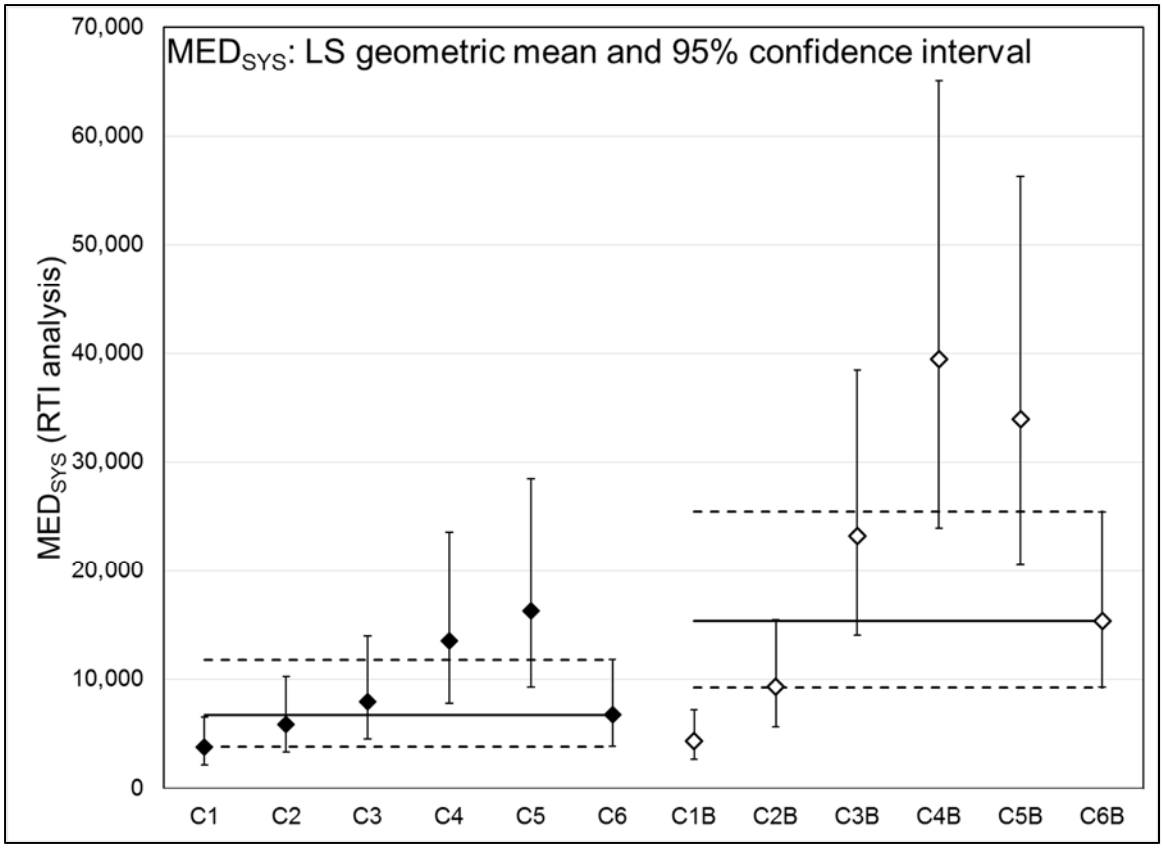

Note: left side (solid points) are for all 23 body regions; right side with the "B" notation (open points) are for the 18 body regions below the neck. LS geometric mean and 95% confidence interval for the C6 configuration are shown as lines for both sets.

Figure 10. LS geometric mean of MED_{SYS} data

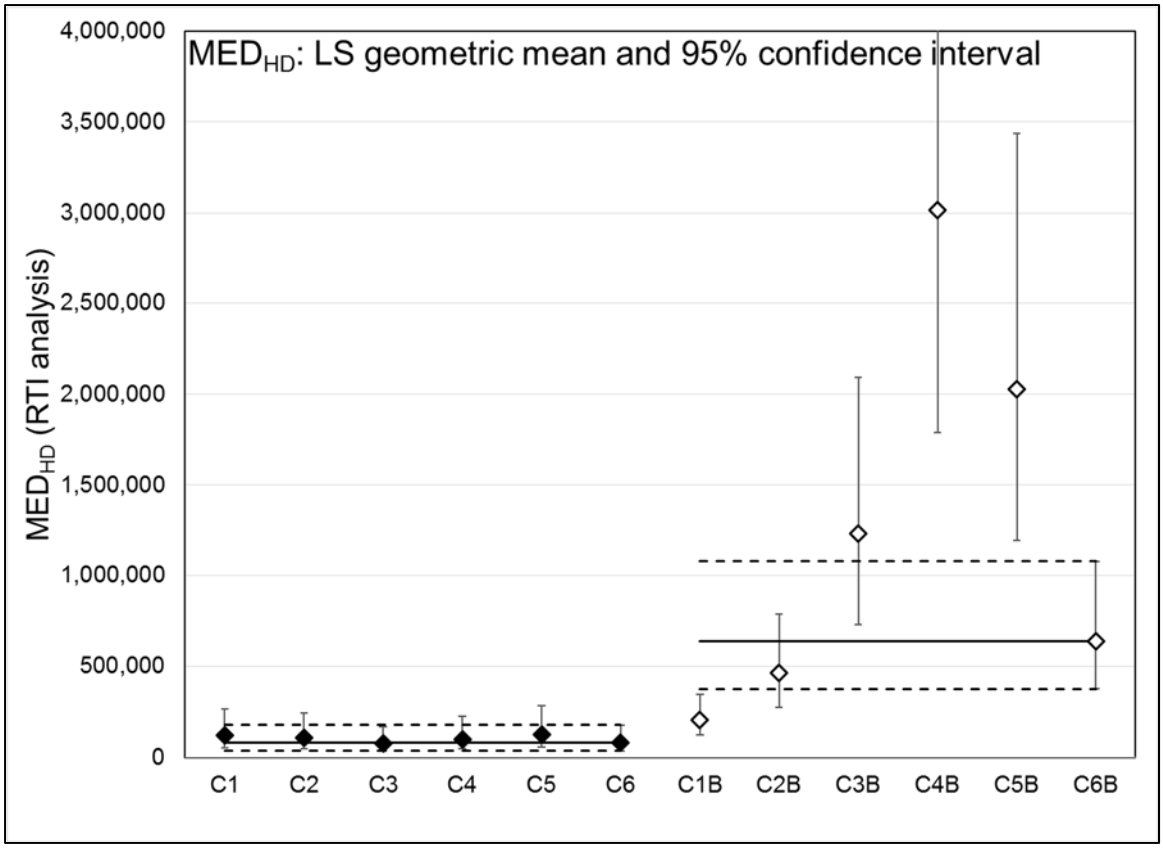

Note: left side (solid points) are for all 23 body regions; right side with the "B" notation (open points) are for the 18 body regions below the neck. LS geometric mean and 95% confidence interval for the C6 configuration are shown as lines for both sets.

Figure 11. LS geometric mean of MED_{HD} data

Similar to the previously presented comparison analysis, where all body regions were considered, the comparison of the MED_{SYS} and MED_{HD} values derived for the below the neck body regions used a Dunnett's test to compare configurations C1 through C5 to a single CB control configuration (C6) but not to each other. The procedure involved hypothesis tests carried out on the log-transformed mean values. If there was no difference between the candidate configuration and the baseline, the calculated estimate would be close to zero, relative to the standard error. The p-values for the hypothesis tests represent the probability of obtaining the measured result or a result more extreme if there really was no difference between the candidate and the baseline. For a statistically significant difference between configurations of 95%, the p-value should be 0.05 or less. The results of this analysis are shown in **Table 18**. For both MED_{SYS} and MED_{HD}, configuration C1 was found to be significantly worse than C6, while configurations C4 and C5 were found to be significantly better than C6.

Table 18. Summary of the IPFS test series ensembles compared to the C6 configuration for the below the neck analysis

Measure	Comparison	Estimate	p-value	Significant difference at 95%?	Better or worse than C6?
Comparison to C6					
MED_{SYS}	C1 to C6	-1.2554	<0.001	Yes	Worse
	C2 to C6	-0.4964	0.211	No	n/a
	C3 to C6	0.4129	0.363	No	n/a
	C4 to C6	0.9430	0.006	Yes	Better
	C5 to C6	0.7930	0.018	Yes	Better
MED_{HD}	C1 to C6	-1.1302	0.002	Yes	Worse
	C2 to C6	-0.3191	0.651	No	n/a
	C3 to C6	0.6590	0.084	No	n/a
	C4 to C6	1.5526	<0.001	Yes	Better
	C5 to C6	1.1556	0.001	Yes	Better

Note: *p*-values less than 0.05 indicate a significant difference at the 95% confidence level.

The below the neck analysis approach allowed statistically significant differences between configurations to be observed for MED_{HD} values, which was not seen when all regions were considered. The same significant differences were observed for both MED_{SYS} and MED_{HD} for the below the neck analysis, which were the same differences observed for MED_{SYS} when all body regions were considered (**Table 14)**. Again, the two layer C4 and C5 configurations showed better aerosol performance, as measured through a BRHA analysis, than the one layer baseline configuration C6.

3.5.6.2 NSRDEC below the neck analysis

Similar to the previous full configuration analysis, three models were considered in comparing the below the neck MED values: Model 1, only configuration as a fixed effect; Model 2, configuration as a fixed effect and test participant as a random effect; and Model 3, both configuration and test participant as fixed effects. Model 2 showed that configuration explained 60% of the variability in the below the neck MED_{HD} data. It was found that Model 3 produced the best model in terms of explaining the variance in the below the neck MED_{HD} and showed that 83% of the total variance can be explained with the configuration explaining 60% and the test participant explaining 28%. Both configuration and test participant had a statistically significant effect on MED_{HD}.

The results from the below the neck MED_{HD} analysis differed significantly from the analysis of the full configuration data. When including the above the neck data, the configuration only explained 5% of the variability in MED_{HD} and was not statistically significant. After removing the head/mask bias, the configuration explained 60% of the variability and was statistically significant. The test participant was statistically significant for both the full configuration and the below the neck data. Also, more variability was explained in the below the neck MED_{HD} than for the full configuration MED_{HD} (83% and 74%, respectively).

3.6 Comparisons of Swatch to System Testing Results

Generally, aerosol swatch testing showed the C3 material to have the highest aerosol filtration efficiency. The C3 Vent material had the highest measured swatch values across the particle size range measured and the C3 Base material contained an air-impermeable layer which, in principle, made this impermeable to any material aerosol penetration. Conversely, the baseline C6 material generally showed the lowest filtration efficiency by the aerosol swatch testing. However, all system comparisons of the BRHA derived parameters between C3 and C6 showed no statistically significant differences between the two configurations. **Figure 12** graphically shows the statistically (95% confidence) better, same, or worse DVs for the different body regions when C3 is compared to C6 (from Appendix C in the Battelle report). While C3 does look like it prevents aerosol deposition in more regions than C6, these occur in regions which have less of an impact on the overall MED_{SYS} and MED_{HD}. Clearly, far better aerosol swatch level results did not lead to better system performance.

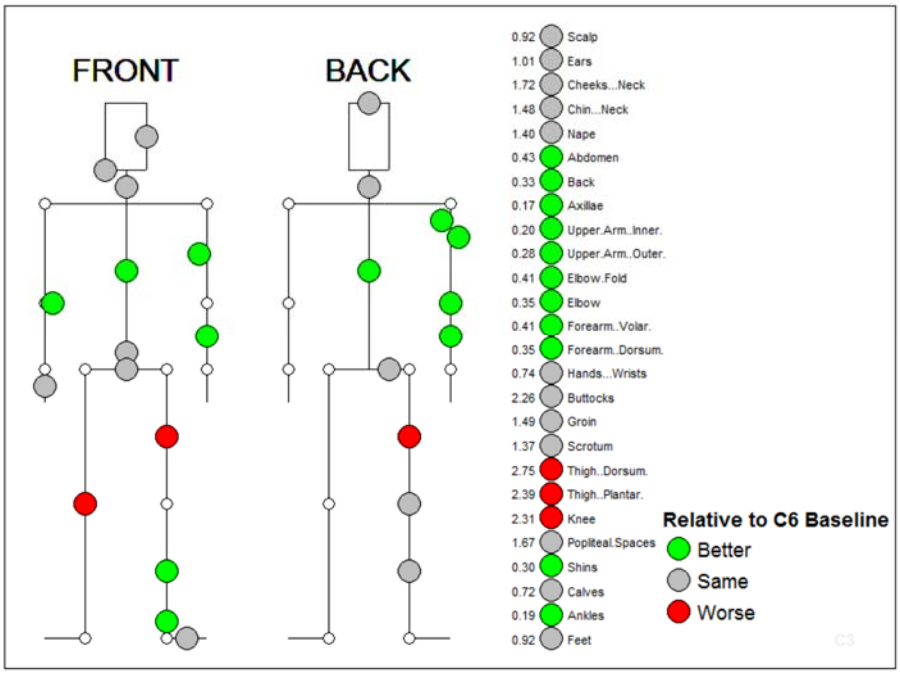

Figure 12. AST DV Results: Ratio of C3 to C6

As another comparison, the C1 (and identical C2) material showed a higher aerosol swatch aerosol filtration efficiency than the C6 material, but the C1 configuration was shown to be significantly worse than the C6 configuration in some of the statistical discussions above for the system tests. The aerosol deposition comparison (see **Figure 8**) shows no region where C1 was better than C6, only similar or worse. Again, in this case, better aerosol filtration efficiencies at the swatch level did not correlate to better system performance.

The Battelle aerosol swatch data in **Table 6** show the C5 material to be somewhere between the filtration efficiencies of the C1 and C6 materials, better than the C6 and somewhat worse than the C1. The aerosol deposition comparison of the C5 configuration with the C6 configuration is

shown in **Figure 13**. There are no regions where C5 is worse than C6 and the C5 configuration was statistically better than the C6 configuration in some of the statistical discussions of the system tests. In this case, the material with the better filtration efficiency was also the better configuration in the system test.

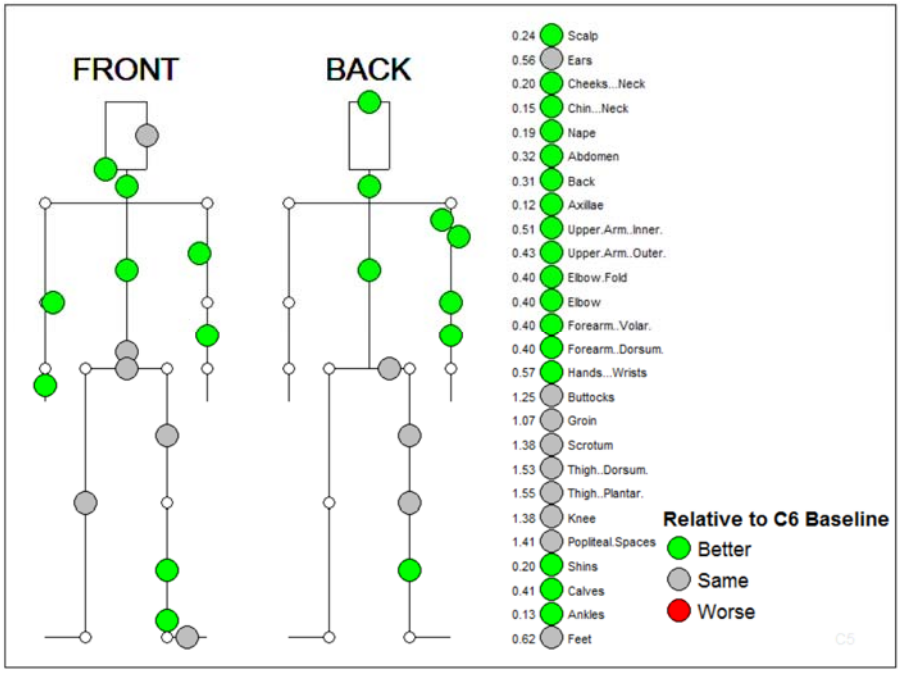

Figure 13. AST DV Results – Ratio of C5 to C6

These three examples do not present a very clear picture of a relationship between swatch aerosol filtration efficiency and aerosol system test performance. In the first case, a much better swatch performance corresponded to indistinguishable system performance differences. In the second case, a better aerosol swatch performance corresponded to a worse system performance. In the third case, a somewhat better swatch performance corresponded to a better system performance

3.7 Comments on Field Wear with Regard to Aerosol Performance

A single laundering was observed to negatively affect the aerosol swatch performance of materials containing an aerosol barrier layer. Also, delamination/abrasion of the aerosol layer was observed during actual field trials of the IPFS configurations where abrasion by the lower leg/boot with the exposed ePTFE of the EFRACU in configuration C4 can be observed (**Figure 14**). There is some evidence that a more robust and thicker aerosol layer may be more durable. Since adhesion also seems to be an issue and polytetrafluoroethylene is notoriously difficult to bond to, other materials for aerosol barriers may improve the physical durability of the aerosol layer adhesion.

Figure 14. Configuration C4 (inner) after field wear from lower leg/boot abrasion

4. CONCLUSIONS

Aerosol swatch measurements showed no correlation to aerosol system performance for the materials and configurations investigated in this study. Limited pressure drop measurements for aerosol swatch tests indicate improved aerosol filtration efficiency with materials with a lower pressure drop than the control configurations.

Good correlation was observed between the NSRDEC and Battelle swatch testing for the small particle range.

Only one configuration material, C3 Vent, met the TTA threshold for aerosol swatch filtration efficiency of 90% for 0.1 μm particles. Swatches for C3 Base could not be measured since the material contains an air-impermeable layer. It is assumed that this would allow no aerosol penetration.

Significant scatter was observed for aerosol deposition between replicate AST trials of the same configuration, leading to large confidence intervals for the derived averages.

It is critical to compare the same data sets with the LS analysis that was applied to determine statistical significance. Different conclusions could be drawn when means and confidence intervals are derived from slightly different data sets.

Statistically significant differences for system performance were observed for whole system MED_{SYS} values from the BRHA analysis. Better aerosol resistance was observed for the two layer C4 and C5 garment configurations when compared to the one layer C6 baseline configuration.

No statistically significant differences were observed for whole system MED_{HD} values from the BRHA analysis for any IPFS configuration when compared to the baseline configurations.

Statistical significance was realized for MED_{HD} values when the mask/hood aerosol deposition was mathematically eliminated from the BRHA calculations. The two layer C4 and C5 garment configurations were significantly better than the C6 baseline configuration for this below the neck analysis.

Modeling of the BRHA derived values showed that a significant amount of the variance can be attributed to the differences in test participants.

5. RECOMMENDATIONS

The lack of correlation between swatch level testing and system testing needs further exploration. While garment design should affect aerosol deposition patterns, the large variations in swatch aerosol filtration efficiency were also expected to lead to identifiable deposition differences between the configurations that could be associated with changes in under ensemble flow.

AST was run with added ballistic gear (aerosol impermeable) on the torso, which may have masked any deposition that could be correlated with swatch level testing. It is recommended that future AST be run with minimal gear that covers the configuration material of interest.

Statistical evaluation of the BRHA data from the AST DVs was found to yield different results depending on the configuration data set included in the computation of the averages. Also, the AST was carried out on an unbalanced design (five replicates with six test participants). Since test participants significantly contributed to the variance, it is recommended that a balanced design be utilized for AST and all statistical analysis be carried out on the same configuration data set.

Durability of thermoplastic-based aerosol layer materials needs to be addressed. Laundering and field wear have clear negative effects on aerosol performance, and it appears due to the thermoplastic susceptibility to debonding and abrasion. Greater durability may be realized with thicker materials, but these may also increase thermal burden. More elastomeric membranes may provide better adhesion and better deformation properties. The aerosol barrier layers should also be protected on both sides with more durable layers. It is recommended that these different approaches to durability be pursued.

This document reports research undertaken at the U.S. Army Natick Soldier Research, Development and Engineering Center, Natick, MA, and has been assigned No. NATICK/TR- 17/021 in a series of reports approved for publication.

6. REFERENCES

McVeety, B., Shumaker, S., Stickel, G., andTew, S., “Final Report Integrated Protective Fabric System Candidate Barrier Materials Chemical Agent and Simulant Testing”, Delivery Order Number: 0779, CBRNIAC Task Number:CB-13-0672, 30 April 2015.

Test Operations Procedure (TOP) 08-2-501A, “Permeation Testing of Materials with Chemical Agents or Simulants (Swatch Testing),” U.S. Army Test and Evaluation Command, August 5, 2013.

Test Operations Procedure (TOP) 10-2-022A, “Chemical Vapor and Aerosol System-Level Testing of Chemical/Biological Protective Suits”, U.S. Army Test and Evaluation Command, December 16, 2013.

Jackson, L., Derringer, G., Steegman, A.T., and Brletich, R., . “Sizing Determination Final Report”, Contractor Report CRDEC-CR-87113 delivered to Chemical Research, Development & Engineering Center, Aberdeen Proving Ground, MD, 1988.

Kierzewski, M.,Mendez, S., andSommerville, D., “Application of Revised Body Region HD Toxicity Estimates to the T&E Body Region Hazard Assessment (BRHA) Methodology”, Edgewood Chemical Biological Center Draft Technical Report, October 2011

IPFS Materials Report (in preparation, to be submitted as NSRDEC Technical Report)

IPFS Materials Manufacturing Report (in preparation, to be submitted as NSRDEC Technical Report)

American Association of Textile Chemists and Colorists (AATCC) Method 135, “Dimensional Changes of Fabrics after Home Laundering”, 2015.

LIST OF ACRONYMS

AFS - Alternative Footwear Solution
ANOVA – analysis of variance
AST – aerosol system test
BRHA – body region hazard analysis
CB – chemical biological
CBCC – Chemical Biological Combat Coverall
CBEC – Chemical Biological Emergency Coverall
CBFRACU - Chemical Biological Flame Resistant Army Combat Uniform
CBRNIAC - Chemical, Biological Radiological & Nuclear Defense Information Analysis Center
CBUG – Chemical Biological Undergarment
CPC - condensation particle counter
Ct – product of concentration multiplied by exposure time
CT_{50} – 50 percent cytotoxicity value (concentration with 50% cell mortality)
DOP – dioctylphthalate
DTIC - Defense Technical Information Center
DV – deposition velocity
EFRACU – Enhanced Flame Resistant Army Combat Uniform
ePTFE – expanded polytetrafluoroethylene
FR – flame resistant
FRACU – Flame Resistant Army Combat Uniform
GFF – glass fiber filter
HD – distilled sulfur mustard
8-HQ/BIT – 8-hydroxyquinoline/benzisothiazol
IOTV – Improved Outer Tactical Vest
IPFS – Integrated Protective Fabric System
JC3 – Joint Chemical Biological Coverall for Combat Vehicle Crewmen
JSLIST – Joint Service Lightweight Integrated Suit Technology
LED – localized exposure dosage
LS – least squares
MED – overall minimum exposure dosage
MED_{HD} – overall local minimum exposure dosage
MED_{SYS} – overall systemic agent minimum exposure dosage
MMD – mass median diameter
NSRDEC – Natick Soldier Research, Development and Engineering Center
PAO - polyalphaolefin
PP - polypropylene
PVAM – polyvinyl amine
RTI – Research Triangle Institute
TOP – Test Operations Procedure
TTA – Technology Transition Agreement
UIPE – Uniform Integrated Protective Ensemble
VX – chemical nerve agent